JOURNAL OF MATERIALS SCIENCE **32** (1997) 4833–4836

Preparation and properties of barium aluminosilicate glass-ceramics

WANCHENG ZHOU, LITONG ZHANG, JUEMING YANG
Northwestern Polytechnical University, Institute of Materials Science and Engineering, Xi'an, Shaanxi 710072, People's Republic of China

Barium aluminosilicate (BAS) glass-ceramics were prepared by hot-pressing BAS glass powder derived via the sol–gel method, and the microstructure and properties were studied. Through control of composition, BAS glass-ceramics with two different types of microstructure were obtained. One is a sub-micrometre celsian surrounded by a thin layer of glassy phase, and the other is a celsian–mullite composite microstructure. BAS glass-ceramics with the celsian–mullite composite microstructure have a strength of 204 MPa and a creep rate of $\leqslant 1.03 \times 10^{-4}\ \mathrm{h}^{-1}$ at 1250 °C. After heat treatment at 1250 °C for 100 h, no significant change of the microstructure was found, and the high-temperature strength did not decrease greatly. The BAS glass-ceramics prove to be a potentially good matrix for fibre- or whisker-reinforced composites for high-temperature applications.

1. Introduction

Glass-ceramic matrix composites have high strength, low cost, and low processing temperature, and are potential candidates for high-temperature structure applications. Barium aluminosilicate (BAS) glass-ceramic is a highly refractory glass-ceramic and has been studied as the matrix of fibre- or whisker-reinforced composites by many researchers [1–7].

Celsian, which has a low thermal expansion and is stable below 1590 °C, is good for the mechanical properties of the composite. When BAS glass crystallizes, however, hexacelsian, a metastable phase that has a high thermal expansion and is harmful to the mechanical properties of the composites, is usually formed, and is hard to transform into the stable celsian [1]. It is thus essential to make celsian, rather than hexacelsian, precipitate out from BAS glasses, or to make the hexacelsian readily transform to celsian.

Drummond [2] prepared BAS glass-ceramics by cold isostatic pressing of melted BAS powder and sintering. The room-temperature strength was in the range 60–120 MPa. Buzniak *et al.* [3] reported that hot-pressed BAS showed rapid degradation of the fracture strength above the glass transition temperature (approximately 900 °C), and that annealing at temperatures above 1000 °C showed a significant increase in the fracture strength at elevated temperatures.

The present work focused on a study of ways to obtain celsian glass-ceramics, to control the microstructure, and to improve the high-temperature mechanical properties.

2. Experimental procedure

The BAS glass powder used in this study was prepared from metal alkoxide through the sol–gel process described elsewhere [8]. Two groups of glass-ceramic samples, celsian glass-ceramic and mullite/celsian glass-ceramic, were prepared in the shape of discs, 60 mm in diameter and 5 mm thick. The celsian glass-ceramic samples were hot-pressed at 1100–1200 °C for 0.5 h with a pressure of 7–15 MPa, and the celsian/mullite glass-ceramic samples were hot-pressed at 1400 °C for 0.5 h with a pressure of 15 MPa. The discs were cut and polished to 3 mm × 4 mm × 40 mm for measurement of bending strength, and to 4 mm × 4 mm × 50 mm for measurement of thermal expansion coefficient. The compositions of the samples are listed in Table I.

The strength and the elastic modulus were measured using the three-point bending test. The elastic modulus was measured at room temperature and the strength was measured at temperatures ranging from 1100–1300 °C, as well as room temperature. The span was 30 mm and the speed of the crosshead was $0.5\ \mathrm{mm\ min^{-1}}$ for measurement of strength and $0.05\ \mathrm{mm\ min^{-1}}$ for measurement of elastic modulus. The strength and elastic modulus of each sample were the averages of 3–5 tests. The creep rate of a typical sample was measured at 1250 °C under a stress of 50 MPa using the three-point bending test. The creep rate was calculated from the moving rate of the cross-head. The method to estimate creep rate from the moving rate of the cross-head is given in the Appendix.

Measurement of the phases in the samples was conducted by X-ray diffraction and the microstructure was studied by scanning electronic microscopy.

3. Results and discussion

3.1. Phase compositions and properties of glass-ceramics with different amounts of Al_2O_3 addition

Table II gives the phase compositions and thermal expansion coefficients of the glass-ceramics. Fig. 1 shows the high-temperature strengths of sample

TABLE I Batch compositions (wt %) of samples

Sample	BaO	Al_2O_3	SiO_2	Additives
A	29	26	45	
A1	29	26	45	+ 10% Al_2O_3 + 5% celsian seeds
A2	29	26	45	+ 22% Al_2O_3 + 5% celsian seeds
A3	29	26	45	+ 34% Al_2O_3 + 5% celsian seeds
B	37	26	37	
B1	37	26	37	+ 5% celsian seeds
B2	37	26	37	+ 1% Li_2O
B3	37	26	37	+ 3% Li_2O
B4	37	26	37	+ 5% Li_2O

TABLE II Phase[a] composition (%) and thermal expansion coefficients (TEC) of BAS glass-ceramics

	M	H	Cel	Cor	Cri	S	G	TEC (10^{-6} °C^{-1})
A	5	87			3		5	7.2
A1	8	17	65	5	2		3	4.2
A2	23	14	52	11				5.1
A3	27	11	47	15				6.4
B	3	95					2	7.4
B1		20	80					4.5
B2		20	80					4.8
B3		5	90			5		2.3
B4		3	87			10		

[a] M, Mullite; H, hexacelsian; Cel, celsian; Cor, corundum; Cri, cristoballite; S, β-spodumene; G, glass phase.

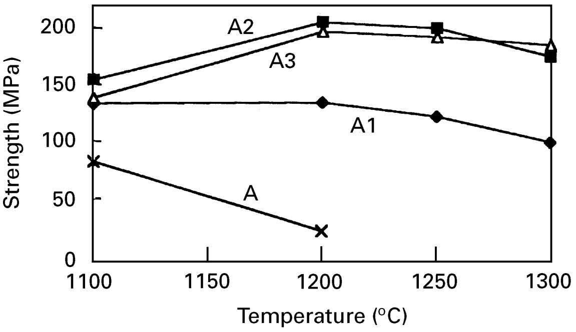

Figure 1 High-temperature strengths of glass-ceramics with different amount Al_2O_3.

series A. It can be seen that, with increasing the amount of Al_2O_3, the amount of mullite increases accompanied by an increase in the high-temperature strength of the glass-ceramics. A2 has a peak strength of 208 MPa at 1200 °C and a strength of 204 MPa at 1250 °C. With the addition of the celsian seed, the major amount of hexacelsian is transformed into celsian, resulting in a decrease of the thermal expansion coefficient. Because the thermal expansion coefficients of both corundum and mullite are greater than that of celsian, the thermal expansion coefficient of the glass-ceramics increases with decreasing celsian and increasing of mullite and corundum contents.

Samples of series A are in the triangle of SiO_2–$BaO \cdot Al_2O_3 \cdot 2SiO_2$–$3Al_2O_3 \cdot 2SiO_2$ in the BaO–Al_2O_3–SiO_2 system (Fig. 2). The equilibrium phases are celsian, mullite and silica. All introduced alumina should be reacted to form mullite and celsian. Because equilibrium has not been achieved in this study, an amount of unreacted alumina (corundum) remains, and its amount increases with the amount introduced. This remaining alumina is beneficial to the high-temperature strength, but detrimental to thermal expansion. The addition of the extra amount of Al_2O_3 also decreases the amount of glass phase, giving rise to the high-temperature strength.

Fig. 3 shows the creep curve of sample A2. The creep curve was obtained through a three-point bending test at a stress of 50 MPa. The tensile creep rate can be estimated to be $\leqslant 1.03 \times 10^{-4}\ h^{-1}$ according to the deflection rate data (the Appendix gives the procedure for estimating tensile creep rate from the deflection rate). This creep rate is low compared with other glass-ceramics. It is believed that fine grains result in poor creep resistance. In the glass-ceramics studied, however, good creep resistance was obtained with a grain size of $\leqslant 0.5\ \mu m$. Microstructure study revealed that the grains in the glass-ceramics formed clusters, and creep proceeded through sliding at the boundary of the clusters. Thus, the clusters acted as coarse grains and resulted in good creep resistance (Fig. 4). The formation of clusters is possible when mullite forms at the boundary of celsian. The mullite links the celsian grains and counteracts the effect of the glassy phase.

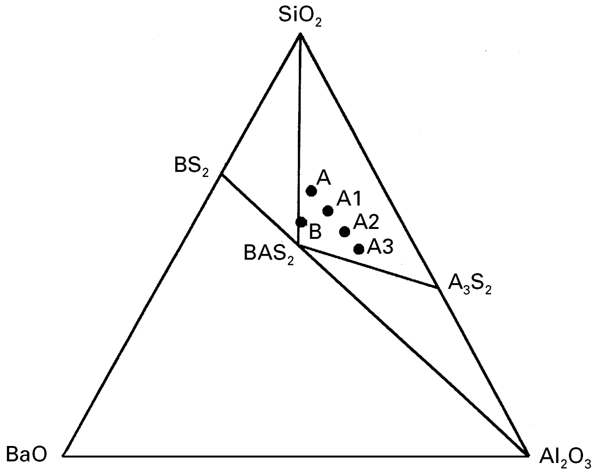

Figure 2 Composition points of series A glass-ceramics in the BaO–Al_2O_3–SiO_2 phase diagram.

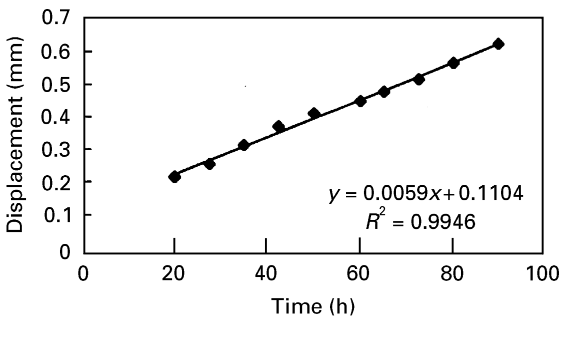

Figure 3 Displacement of the crosshead with time at steady-state creep of A2 at 1250 °C under a stress of 50 MPa.

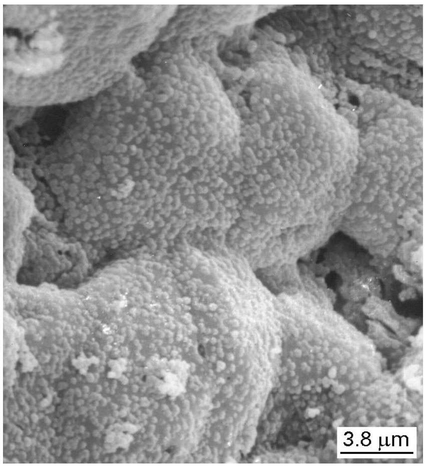

Figure 4 Microstructure of a mullite/celsian glass-ceramic sample showing clusters of grains after the creep test.

3.2. Effect of lithium oxide on high-temperature strengths and thermal expansion

Fig. 5 shows the effects of lithium on the room-temperature and high-temperature strengths of celsian glass-ceramics. As the amount of Li_2O increases, the room-temperature strength changes little, while the strength at 1200 °C is more affected. A small amount of Li_2O is beneficial to the high-temperature strength of the glass-ceramics, while the high-temperature strength is dramatically decreased at Li_2O contents higher than 1 wt %. X-ray analysis revealed that β-spodumene was formed when 3 wt % or more Li_2O was added to the glass-ceramics, which lowered the thermal expansion coefficients of the glass-ceramics, and at the same time, decreased the high-temperature strengths.

By comparing the thermal expansion coefficients of B, B2, and B3 in Table II, it can be seen that the addition of Li_2O effectively reduces the thermal expansion coefficient of the glass-ceramics. A small amount of Li_2O decreases the thermal expansion of the glass-ceramics by converting hexacelsian into celsian, and a large amount of Li_2O works by forming β-spodumene which has a very low thermal expansion coefficient.

3.3. Effect of other factors on the high-temperature strengths

Fig. 6 shows the high-temperature strengths of samples A, B, B1, and B2. The main crystalline phases of both A and B are hexacelsian. The composition of sample A is not as close to the theoretical composition of $BaO \cdot Al_2O_3 \cdot 2SiO_2$ as sample B, and thus contains a small amount of cristoballite and glass phase, while sample B does not contain cristoballite and the amount of glass phase B is less. This phase composition gives sample B a better strength.

Sample B1 has essentially the same composition as sample B. Because the addition of the 5 wt % celsian seed transforms most of the hexacelsian into celsian, the main difference between samples B and B1 is the main crystalline phase. The higher strengths of B1 than those of B over the whole temperature range shown in Fig. 6, indicate that glass-ceramics with celsian as the main crystalline phase have higher strengths than those with hexacelsian as the main crystalline phase. Sample B2 also has the same composition, except for the 1 wt % Li_2O. The addition of Li_2O converts most of the hexacelsian into celsian, and increases the high-temperature strengths. Samples B1 and B2 have essentially the same phase composition (Table II), but B2 has clearly higher strengths over the whole temperature range. This can probably be attributed to the molecular-level mixing of the Li_2O in B2, while the celsian seed in B1 cannot be mixed at such a level.

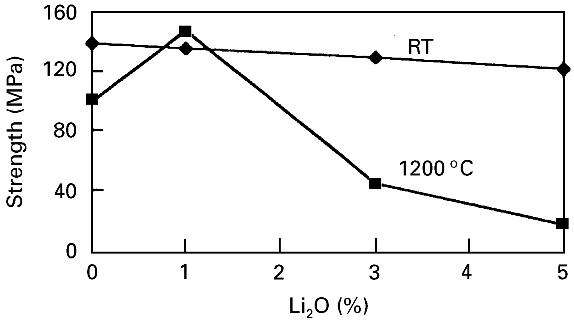

Figure 5 The effect of Li_2O content on the strength of the celsian glass-ceramics.

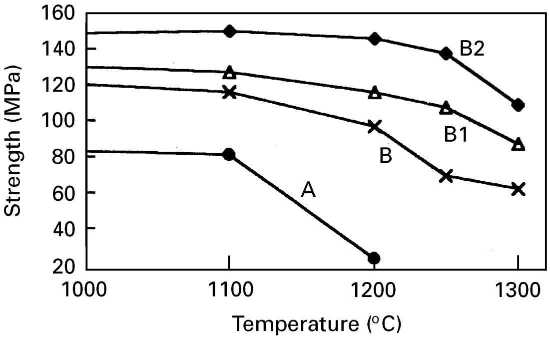

Figure 6 High-temperature strengths of celsian and hexacelsian glass-ceramics (phase compositions are shown in Table II).

4. Conclusion

Glass-ceramics in the $BaO–Al_2O_3–SiO_2$ system have been prepared by hot-pressing from glass powders derived via the sol–gel method. Both the chemical compositions and the phase compositions have important effects on the strengths and thermal expansion coefficients of the glass-ceramics. The addition of an extra amount of alumina produces mullite in the glass-ceramics, which counteracts the effect of glass phase and increases the high-temperature strengths. As mullite has a higher thermal expansion coefficient than celsian, the increase in the amount of mullite increases the thermal expansion coefficient of a celsian–mullite glass-ceramic. Celsian is preferable to hexacelsian, for high strength and low thermal expansion. The addition of celsian seeds and Li_2O into the glass-ceramics is effective in converting hexacelsian into celsian, but too much Li_2O severely decreases the high-temperature strengths.

Appendix. Estimation of creep rate from the deflection rate in the bending test

We assume that: (1) the displacement of the crosshead or the deflection is very small compared to the length of the beam sample; (2) the cross-section of the beam sample maintains its rectangular shape before and after deformation; (3) the bending deformation causes the length of the beam at the upper side to become shorter, that at the lower side to become longer, and that at the middle height remains unchanged (Fig. A1).

At steady-state creep, the relationship between the strain, ε, the stress, σ, and the creep time, t, can be expressed as

$$\varepsilon = A\sigma^{\alpha}t^{n} \tag{A1}$$

where A, α, and n are constants.

From Fig. A1, we obtain $R\theta = \mathrm{d}x$, $(R + h/2)\theta = \mathrm{d}x + i$. Thus, we have

$$\varepsilon = i/\mathrm{d}x = h/(2R) \tag{A2}$$

where R is the curvature radius, h is the height of the beam.

For a given curve, the radius of curvature can be expressed as

$$R = \left[1 + \left(\frac{\mathrm{d}y}{\mathrm{d}x}\right)^{2}\right]^{\frac{3}{2}} \Big/ \frac{\mathrm{d}^{2}y}{\mathrm{d}x^{2}} \tag{A3}$$

Because the deflection is very small compared to the length of the beam, the absolute value of $\mathrm{d}y/\mathrm{d}x$ for any x in the beam will be very small. Thus $(\mathrm{d}y/\mathrm{d}x)^2 \ll 1$, and $[1 + (\mathrm{d}y/\mathrm{d}x)^2] \approx 1$. Equation 3 can be simplified to

$$\mathrm{d}^{2}y/\mathrm{d}x^{2} = 2\varepsilon/h = 2A\sigma^{\alpha}t^{n}/h \tag{A4}$$

where σ is the stress at the lower edge of the beam.

According to the above hypotheses, the creep is very small and can be treated as elastic deformation. Therefore, σ and x have a linear relationship, $\sigma = kx$, where

$$k = \frac{p(1 + 2\alpha)}{b\alpha h^{2}} \tag{A5}$$

p is the applied load, and b and h are the width and the height of the beam, respectively. Thus

$$\mathrm{d}^{2}y/\mathrm{d}x^{2} = 2Akx^{\alpha}t^{n}/h \tag{A6}$$

Through integration of Equation A6, considering that $y = 0$ at $x = 0$ and $\mathrm{d}y/\mathrm{d}x = 0$ at $x = L/2$, we can obtain

$$y = \frac{2Ak^{\alpha}t^{n}}{h(\alpha + 1)}\left[\frac{x^{\alpha+2}}{\alpha + 2} - \left(\frac{L}{2}\right)^{\alpha+1} x\right] \tag{A7}$$

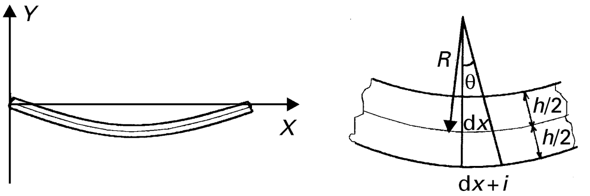

Figure A1 Schematic drawing of a creep-deformed beam.

At $x = L/2$, $y = y_{\mathrm{m}}$ and $\varepsilon = \varepsilon_{\mathrm{m}}$. Thus

$$\varepsilon_{\mathrm{m}} = (A(kL/2)^{\alpha}t^{n} \tag{A8}$$

$$y_{\mathrm{m}} = \frac{L^{2}\varepsilon_{\mathrm{m}}}{2h(\alpha + 2)} \tag{A9}$$

$$\frac{\mathrm{d}\varepsilon_{\mathrm{m}}}{\mathrm{d}t} = \frac{2h(\alpha + 2)}{L^{2}}\frac{\mathrm{d}y_{\mathrm{m}}}{\mathrm{d}t} \tag{A10}$$

$\mathrm{d}y_{\mathrm{m}}/\mathrm{d}t$ can be measured by experiment. If the constant α is known, the creep rate can be estimated from $\mathrm{d}y_{\mathrm{m}}/\mathrm{d}t$. From Equations A8 and A9 we have

$$\begin{aligned}\frac{\mathrm{d}y_{\mathrm{m}}}{\mathrm{d}t} &= \frac{L^{2}}{2h(\alpha + 2)}\frac{\mathrm{d}\varepsilon_{\mathrm{m}}}{\mathrm{d}t}\\ &= \frac{L^{2}}{2h(\alpha + 2)}nA(kL/2)^{\alpha}t^{n-1}\end{aligned} \tag{A11}$$

At steady-state creep, we have $n = 1$. Because the creep deformation of the beam is very small, we can treat it as elastic deformation, in which $A = 1/E$, where E is the elastic modulus. From Equations A5 and A11 we have

$$\frac{\mathrm{d}y_{\mathrm{m}}}{\mathrm{d}t} = \frac{L^{2+\alpha}}{2h(\alpha + 2)E}\left[\frac{p(1 + 2\alpha)}{2b\alpha h^{2}}\right]^{\alpha} \tag{A12}$$

Thus, the constant α can be estimated from Equation A12, and the steady-creep rate, $\mathrm{d}\varepsilon_{\mathrm{m}}/\mathrm{d}t$, can be estimated from Equation A10.

References

1. N. P. BANSAL and M. J. HYATT, *J. Mater. Res.* **4** (1989) 1257.
2. C. H. DRUMMOND III, *Ceram. Engng Sci. Proc.* **11** (1990) 1072.
3. J. J. BUZNIAK, K. P. D. LAGERLOF and N. P. BANSAL, *Ceram. Trans.* **38** (1993) 789.
4. V. S. R. MURTHY and M. H. LEWIS, *Trans. J. Br. Ceram. Soc.* **89**(5) (1990) 173.
5. J. C. DEBSIKDAR, *Ceram. Engng Sci. Proc.* **14** (1993) 405.
6. I. LEE and J. COVINO, *Mater. Res. Bull.* **29** (1994) 55.
7. J. J. BRENNAN and G. McCARTHY, *Mater. Sci. Engng A* **A162**(1–2) (1993) 53.
8. J. YANG, L. ZHANG and W. ZHOU, in "Proceedings of the 17th International Congress on Glasses", Vol. 4, edited by Gong Fangtian (International Academic Publishers, Beijing, 1995) pp. 308–13.

Received 5 July
and accepted 13 November 1996